Electronic Supplementary Material (ESI) for Journal of Materials Chemistry C.

Ultra-Broadening Near-Infrared Emission of Cr^{3+}-Activated Pyroxene Phosphor via Chemical Unit Substitution and Yb^{3+} Co-doping

Shuofeng Sun, Yuming Yang, Renfei Zhang, Qinan Mao*, Lang Pei, Junhua Xi, Yang Ding, Yiwen Zhu, Hua Yu, Jiasong Zhong*

Center for Advanced Optoelectronic Materials & College of Materials and Environmental Engineering, Hangzhou Dianzi University, Hangzhou 310018, People's Republic of China

* Corresponding authors:

Qinan Mao, E-mail: maoqinan@hdu.edu.cn

Jiasong Zhong, E-mail: jiasongzhong@hdu.edu.cn

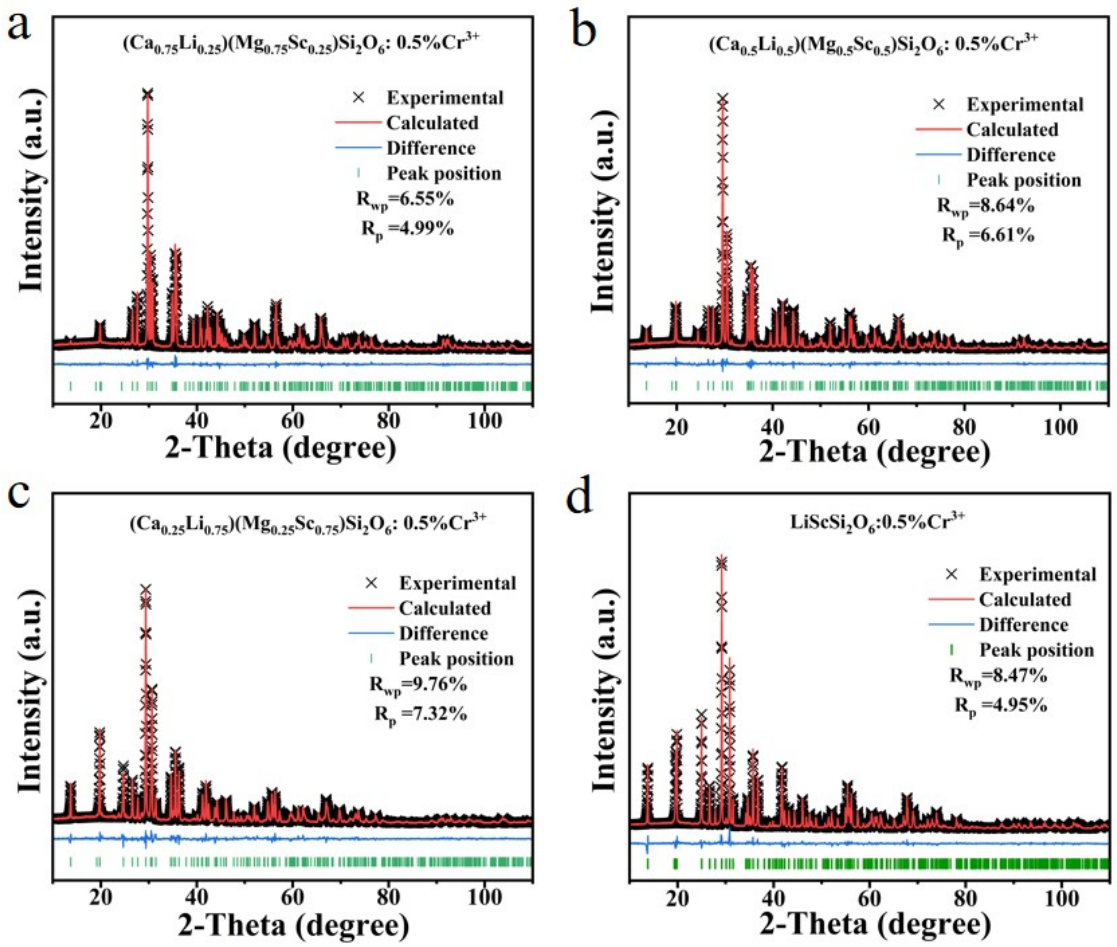

Figure S1. XRD Rietveld refinements of $(Ca_{1-x}Li_x)(Mg_{1-x}Sc_x)Si_2O_6$: 0.5%$Cr^{3+}$ (x=0.25~1) phosphors.

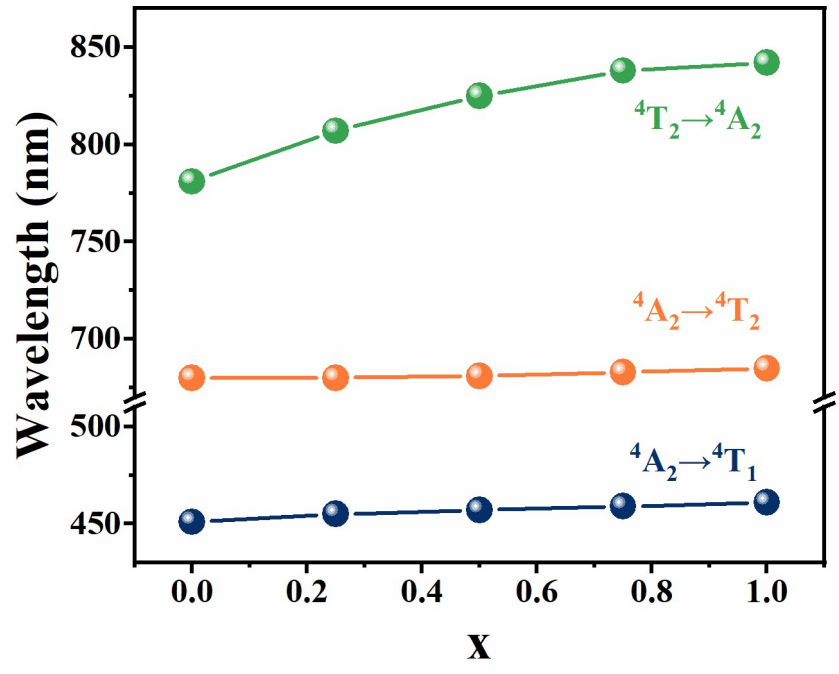

Figure S2. Peak positions of $^4A_2 \rightarrow {}^4T_1$, $^4A_2 \rightarrow {}^4T_2$ and $^4T_2 \rightarrow {}^4A_2$ transitions in $(Ca_{1-x}Li_x)(Mg_{1-x}Sc_x)Si_2O_6$:0.5%$Cr^{3+}$ (x=0~1) phosphors.

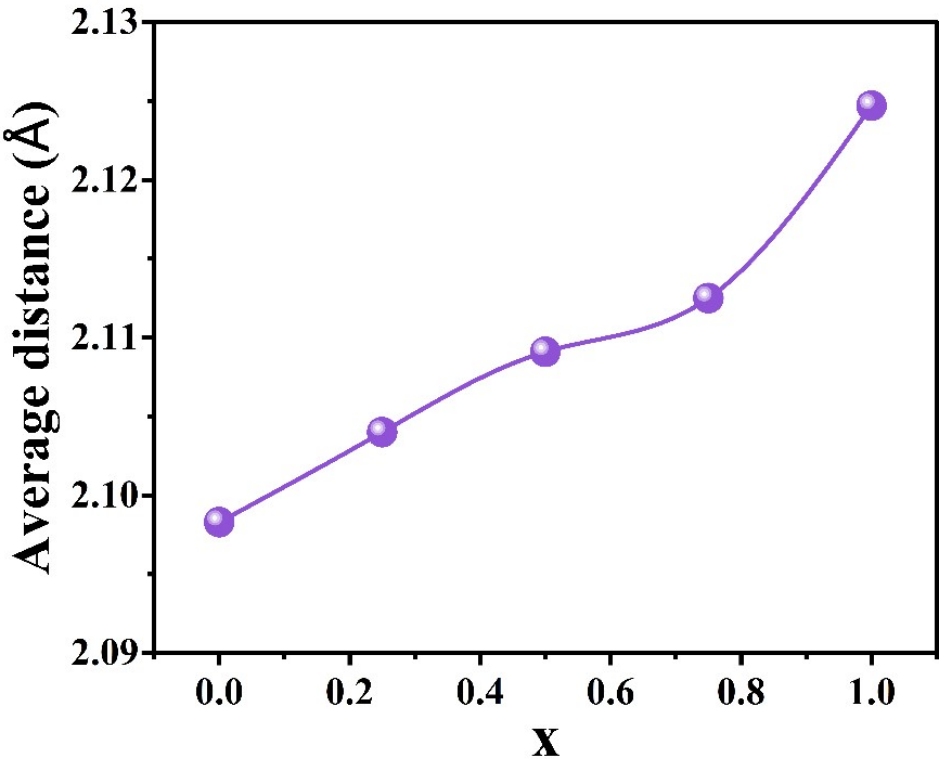

Figure S3. Variation of average bond length of Mg^{2+}/Sc^{3+}-O^{2-} with x for $(Ca_{1-x}Li_x)(Mg_{1-x}Sc_x)Si_2O_6$:0.5%$Cr^{3+}$ (x=0~1) phosphors.

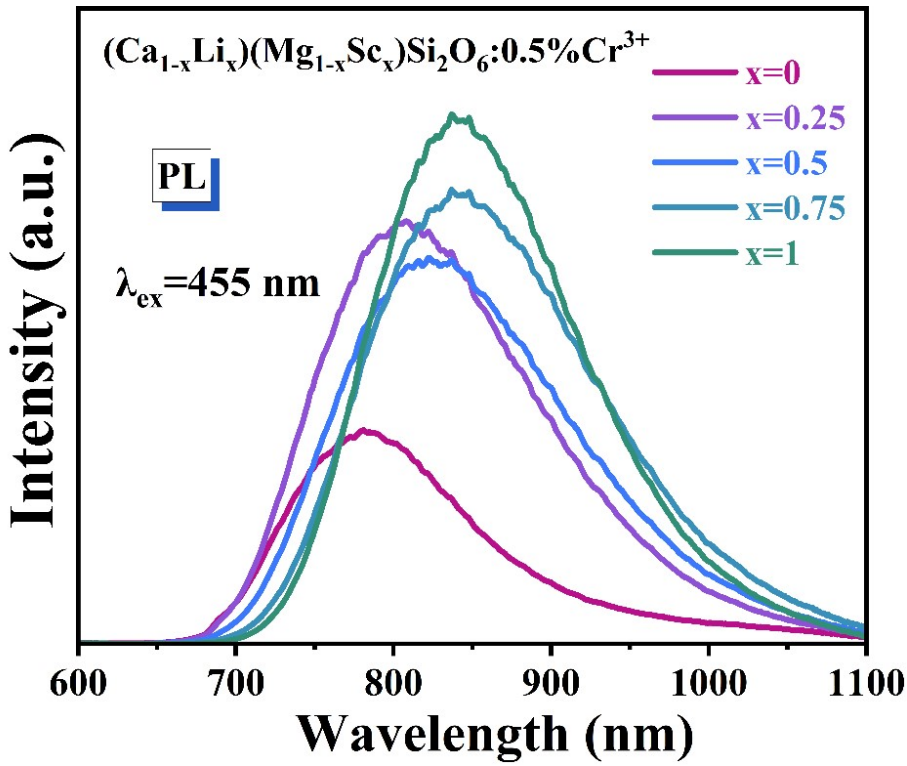

Figure S4. Photoluminescence spectra of $(Ca_{1-x}Li_x)(Mg_{1-x}Sc_x)Si_2O_6$:0.5%$Cr^{3+}$ (x=0~1).

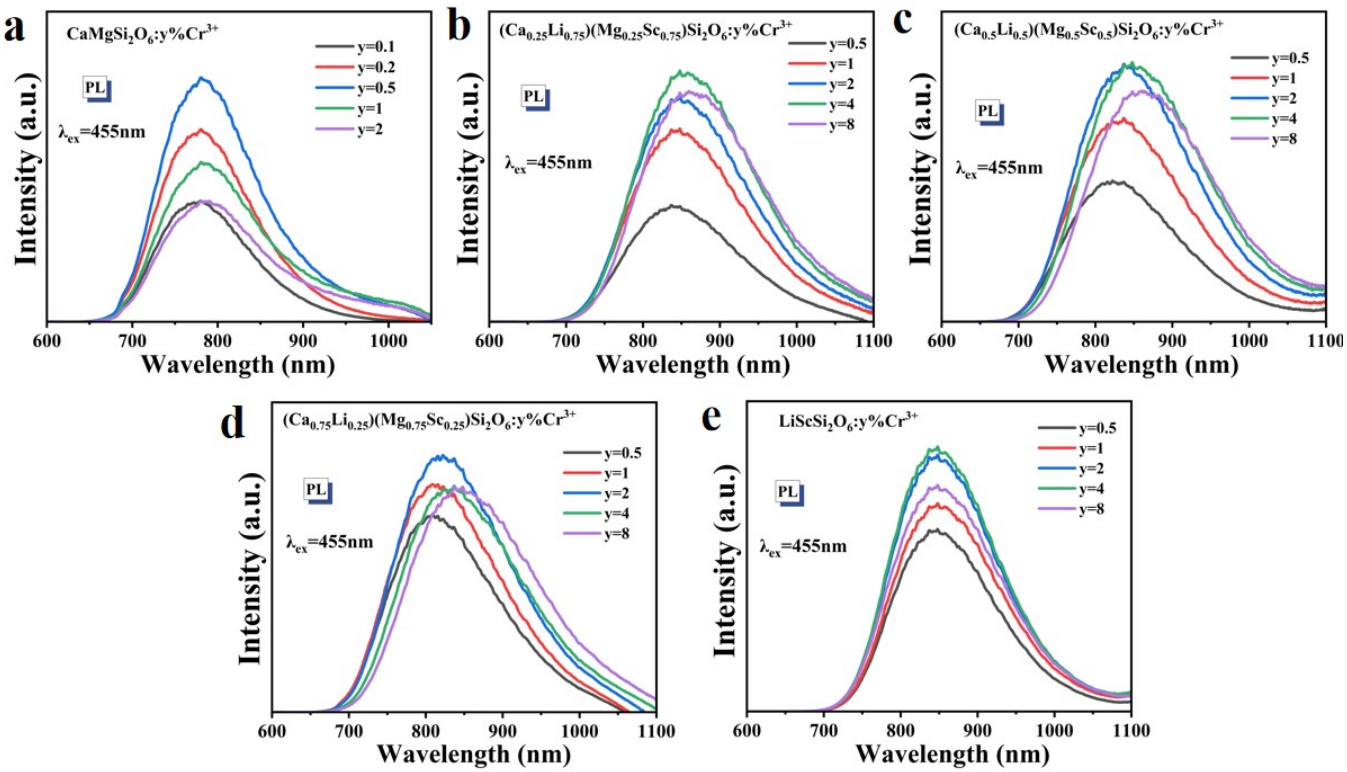

Figure S5. Photoluminescence spectra of $(Ca_{1-x}Li_x)(Mg_{1-x}Sc_x)Si_2O_6:Cr^{3+}$ (x=0~1) with different Cr^{3+} doping concentration.

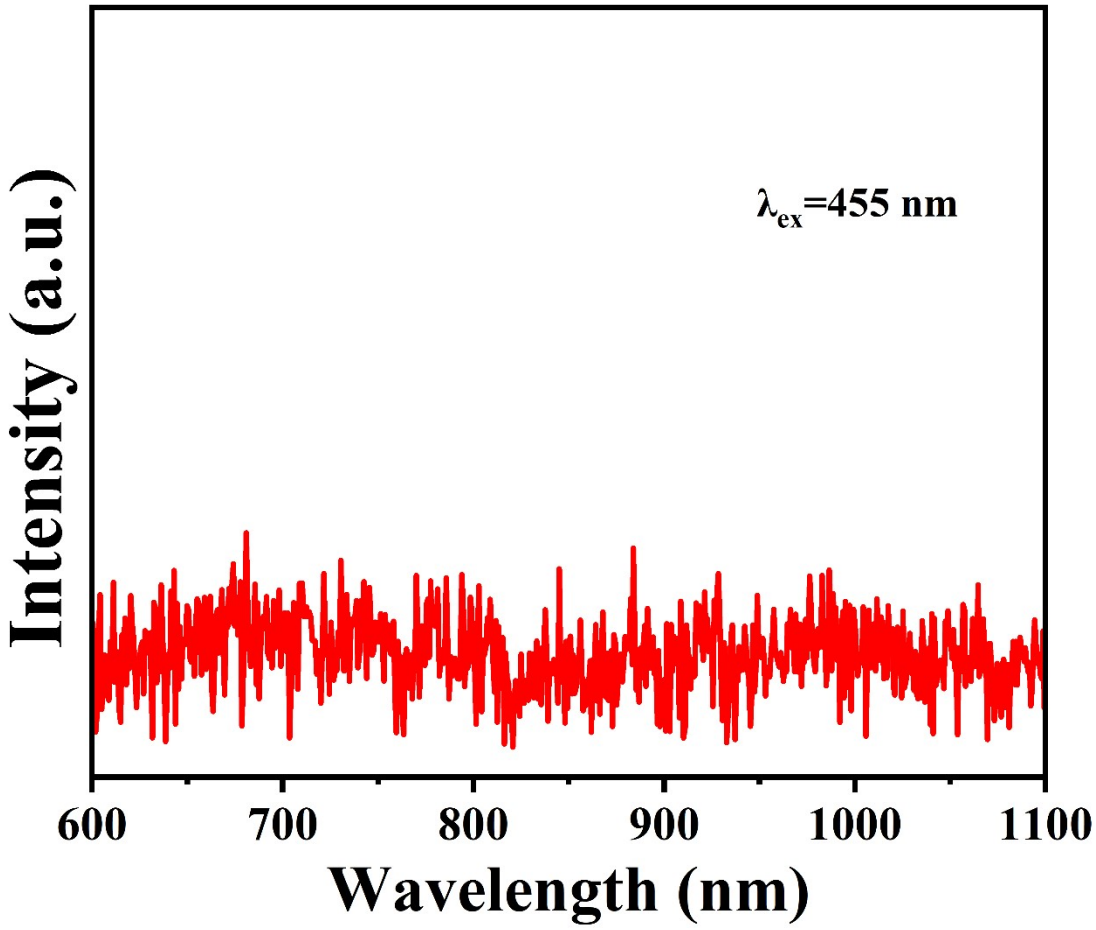

Figure S6. Photoluminescence spectra of $(Ca_{0.5}Li_{0.5})(Mg_{0.5}Sc_{0.5})Si_2O_6:Yb^{3+}$ under 455nm excitation.

Quantum Yield

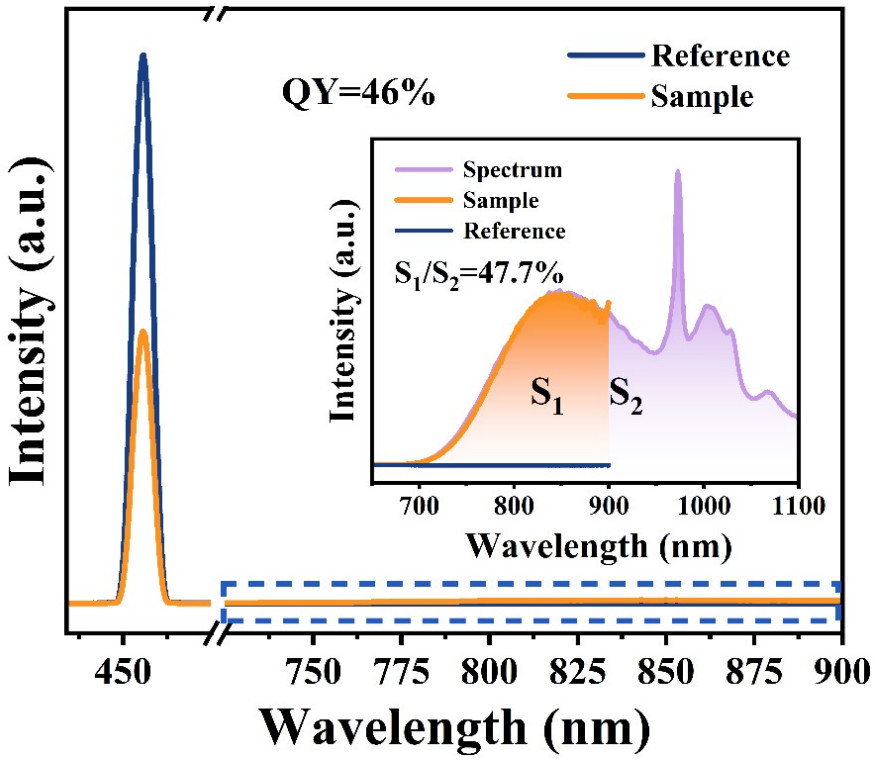

Figure S7. Luminescent spectra for the QY measurement of $(Ca_{0.5}Li_{0.5})(Mg_{0.5}Sc_{0.5})Si_2O_6$:4%$Cr^{3+}$,0.4%$Yb^{3+}$

The value of internal QY is calculated from the following equation [1]:

$$QY = \frac{\int L_S - \int L_R}{\int E_R - \int E_S} \times 100\%$$

where L_S and L_R are the luminescent spectrum of the sample and the $BaSO_4$ reference, respectively; E_S and E_R are the excitation light spectra of the sample and the $BaSO_4$ reference, respectively. Due to the spectral response of VIS PMT detector, the measurement of QY was recorded spanning from 650nm to 900 nm. As shown in Fig

S6, the calculated QY of emission in orange area (S_1) is 21.92%. The area ratio of S_1 (integral area from 650 nm to 900 nm) to S_2 (integral area from 650 nm to 1100 nm) is 47.7%. Therefore, the QY of $(Ca_{0.5}Li_{0.5})(Mg_{0.5}Sc_{0.5})Si_2O_6$:4%$Cr^{3+}$,0.4%$Yb^{3+}$ phosphor is determined to be above 46%.

Table S1. The detailed refinement results of $(Ca_{1-x}Li_x)(Mg_{1-x}Sc_x)Si_2O_6:Cr^{3+}$ (x=0~1) phosphors

	x=0	**x=0.25**	**x=0.5**	**x=0.75**	**x=1**
a(Å)	9.7903	9.7722	9.7570	9.7445	9.7471
b(Å)	8.9348	8.9433	8.9509	8.9416	8.9381
c(Å)	5.3550	5.3468	5.3283	5.2946	5.2714
V(Å^3)	439.379	439.860	440.727	440.547	440.612
α (°)	90.000	90.000	90.000	90.000	90.000
β (°)	105.917	106.378	107.262	108.719	110.284
γ (°)	90.000	90.000	90.000	90.000	90.000
R_{wp}(%)	7.69	6.55	8.64	9.76	8.47
R_p(%)	5.44	4.99	6.61	7.32	4.95
χ^2	2.51	1.75	2.16	3.26	2.93

Table S2. The calculated values of crystal field splitting parameter (Dq) and Racah parameter (B)

	x=0	**x=0.25**	**x=0.5**	**x=0.75**	**x=1**
Dq (cm^{-1})	1375	1355	1340	1329	1324
B (cm^{-1})	886	854	845	842	831

The crystal field parameter (*Dq*) and the Racah parameter (*B*) are calculated from the following equations [2]:

$$\Delta E = E\left({}^4A_{2g} \rightarrow {}^4T_{1g}\right) - E\left({}^4A_{2g} \rightarrow {}^4T_{2g}\right)$$

$$\Delta S = E\left({}^4A_{2g} \rightarrow {}^4T_{2g}\right) - E\left({}^4T_{2g} \rightarrow {}^4A_{2g}\right)$$

$$10Dq = E({}^4A_{2g} \rightarrow {}^4T_{2g}) - \frac{\Delta S}{2}$$

$$\frac{D\mathrm{q}}{B} = \frac{15 \times (\frac{\Delta E}{D\mathrm{q}} - 8)}{(\frac{\Delta E}{D\mathrm{q}})^2 - \frac{10\Delta E}{D\mathrm{q}}}$$

where $E({}^4A_{2g} \rightarrow {}^4T_{1g})$ and $E({}^4A_{2g} \rightarrow {}^4T_{2g})$ are the energy values at the excitation peaks of the ${}^4A_2 \rightarrow {}^4T_1$ and ${}^4A_2 \rightarrow {}^4T_2$ transitions, respectively; $E({}^4T_{2g} \rightarrow {}^4A_{2g})$ is the energy value at the emission peak of ${}^4T_2 \rightarrow {}^4A_2$ transition.

References

[1] Yao, L.; Shao, Q.; Shi, M.; Shang, T.; Dong, Y.; Liang, C.; He, J.; Jiang, J. Efficient ultra-broadband Ga_4GeO_8: Cr^{3+} phosphors with tunable peak wavelengths from 835 to 980 nm for NIR pc-LED application. *Adv. Opt. Mater*. 2022, 10, 2102229.

[2] Yuan, C.; Li, R.; Liu, Y.; Zhang, L.; Zhang, J.; Leniec, G.; Sun, P.; Liu, Z.; Luo, Z.; Dong, R.; Jiang, J. Efficient and broadband $LiGaP_2O_7$: Cr^{3+} phosphors for smart near-infrared light-emitting diodes. *Laser Photonics Rev.* 2021, 15, 2100227.